IOP Conf. Series: Materials Science and Engineering **779** (2020) 012026 doi:10.1088/1757-899X/779/1/012026

Study of an inducer and axial vortex stage

A Ankudinov[1], D Klimenko[2], S Timushev[2,3] and A Regeda[1]

[1]Bauman Moscow State Technical University
[2]MAI (Moscow Aviation Institute)

[3]E-mail: irico.harmony@gmail.com

Abstract. Increasing the intake capacity and reducing vibration loads of high-speed pumps is an important task in the development of power systems in the aerospace industry, as well as in the application of such pumps in the energy and oil production sectors. With an improvement in cavitation qualities, pumps can operate at a higher shaft speed, and at a given shaft speed, with lower net positive suction head, that is, at reduced inlet pressure. With increasing shaft speed, the dimensions and weight of the pumps decrease. To increase the cavitation qualities of the pumps, an axial vortex stage (AVS), which is an object of comparison with the inducer, is considered as an upstream device. It is necessary to study the fact of pressure pulsations decrease when using the AVS. The results obtained with computational fluid dynamics to analyze pressure pulsations in the inducer and in the AVS are used in this article.

Introduction

Increasing the requirements for the characteristics of centrifugal pumps: cavitation qualities, reliability, the absence of low-frequency pulsations, the stability of operation in off-design modes, necessitate the search for means for their further improvement. The methods for improving the cavitation qualities of centrifugal pumps are known: the implementation of the first stage centrifugal impeller with an increased neck area at the inlet; the use of a booster pump with a lower shaft speed than the main pump; installation of an upstream jet pump; the use of an inducer. Most often, in order to improve cavitation qualities, an upstream axial screw impeller — an inducer, is installed at the entrance to the first stage centrifugal impeller. However, with good cavitation qualities, an inducer has significant disadvantages. When an inducer operates at flow rates less than 50% of the optimum, back flows are formed, amplifying with decreasing flow rate. The formation of back flows leads to increased vibration, unstable operation on the stall branch of the cavitation characteristic, low-frequency pressure pulsations. One of the promising ways to improve the cavitation qualities of the pump, reduce noise, vibration and low-frequency pulsations is to install the axial-vortex stage at the pump inlet [1]

An axial-vortex stage (AVS) has certain advantages over an inducer: a higher head coefficient, better cavitation qualities, and stability of work at low flow rates [2–4]. Experimental data show that the use of AVS reduces the level of pressure pulsations and vibrations. All these properties of the AVS determine the prospects of its use as an upstream stage of a centrifugal pump.

AVS is a pump consisting of an axial screw and a fixed helical cascade located on its periphery, the of the vanes of which is opposite to the agles of the blades of the screw. The fluid flow in the AVS [5] has a complex tree-dimensional character with a vortex flow at the periphery. Simplistically, the entire flow can be divided into two zones: the main axisymmetric flow located near an inducer hub, and the vortex flow in the peripheral part of the axial screw inducer and in the fixed helical cascade.

The results of experimental studies of AVS

Tests of the AVS models [4–6] were carried out at various shaft speed with different geometry of the flow part. The tested AVS had a relative axial length $\bar{l} = l / D_s = 0,79 - 2,12$ and a relative diameter of the fixed helical cascade $\overline{D_p} = D_p / D_s = 1,11 - 1,33$; hub ratio $\overline{d_{sl}} = d_{sl} / D_s = 0,33 - 0,69$; the angles of installation of the inducer blades along the outer diameter of the inducer were $\beta_s = 8 - 15°$ and of fixed helical cascade were $\beta_g = 8 - 13°$.

The models were tested with a different shape of the inlet edge, a radial clearance between the inducer and the fixed helical cascade assembly, with a variable inducer hub and a variable pitch of its blades.

Fig. 1 shows the performance curves of several variants of AVS with different axial lengths.

For comparison with the performance curves of the AVS on the same graph shows the performance curve of the inducer with the same geometry, which does not have a fixed cascade on the periphery. The performance curves of the inducer without a fixed cascade, differing only in axial length were also studied. The inducer length was $l_s = 256$ mm; 400 mm; 200 mm; 150 mm. The performance curves of the inducer without a fixed cascade practically did not change when the axial length changed. It should be also noted that the head of the inducer without a fixed cascade at the periphery (variant 4) is significantly lower than the pressure of the AVS. The maximum flow rate of all variants, including a conventional inducer, has one value, which corresponds to the flow rate of an shocklessflow input to the inducer blades.

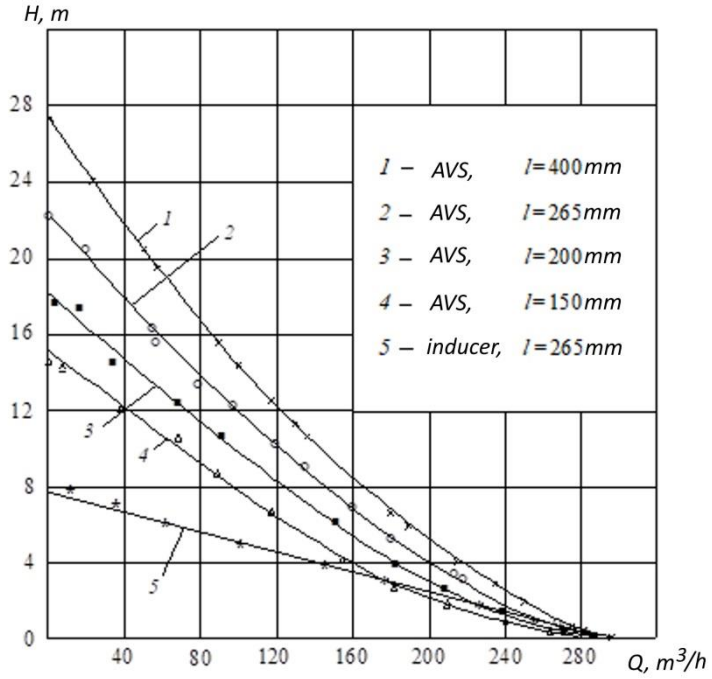

Fig. 1. The performance curves of the AVS with different axial inducer length, n=1500 rpm

Starting from the relative length, which corresponds to a length equal to the diameter of the inducer $\bar{l} = l / D_s = 1$, the pressure coefficient ψ of the AVS variants from the relative axial length when flow rate equal to zero increases almost linearly. This AVS property is similar to the characteristics of labyrinth pumps [7]. The use of AVS makes it possible to obtain the required head, increasing only the axial length. It allows having operating parameters in a larger range than for axial screws that do not have a fixed helical cascade on the periphery, at the same shaft speed.

The experiment confirmed the selected physical model of the AVS and the assumption that the head should increase with increasing mass of the fluid taking part in the secondary flow.

According to the accepted flow model, the theoretical head is proportional to the mass of the secondary flow taking part in the vortex interaction. The mass of the secondary stream depends both on the axial length and on the height of the blades of the movable and fixed helical cascade.

The pressure coefficient of the AVS for the variants $\overline{D_p} = D_p / D_s = 1{,}11; 1{,}22; 1{,}33$ of the fixed cascade changes linearly with the relative diameter at zero flow rate.

To study the development of cavitation in the AVS, visual studies were carried out to determine the nature and direction of the flow in the channels, various stages of the development of cavitation were noted. Fig. 2 is photograph of the fluid flow in the AVS channels under stroboscopic illumination with developed cavitation in the channels.

Fig.2. Fluid flow with developed cavitation in the channels.

The presented results of researches confirm the selected flow model, consisting of the main axisymmetric flow and the secondary vortex flow, on the periphery of the inducer and in the fixed channels.

As it was established in experimental studies, in the axial vortex stage in all operation modes of NPSH, there are no low-frequency pressure pulsations, with the development of cavitation, the levels of pulsation and vibration decrease. It is explained by the fact that the cavitation cavities are localized in a vortex core located in the central part of the helical channels. The collapse of the caverns does not occur on the walls of the casing and blades, as in an ordinary inducer, but in a fluid flow. With decreasing pressure, the volume of cavitation cavities increases. A vortex cavitation core extends over fixed channels over a greater distance, which leads to intense damping of pulsations in the liquid and reduces the vibration level.

Computational fluid dynamics methods

Nowadays, the use of computational fluid dynamics methods for analyzing and optimizing the pumps flow part [8–13] is being standard for engineers. Numerical simulation using computational fluid dynamics methods makes it possible to analyze the influence of the unsteady distribution of parameters in the inducer and AVS on the amplitude and spectrum of pressure pulsations. The model uses the continuity and Navier-Stokes (1,2)equations:

$$\frac{\partial \rho}{\partial t} + \nabla(\rho V) = 0 \tag{1}$$

$$\frac{\partial \rho \cdot V}{\partial t} + \nabla(\rho \cdot V \times V) = -\nabla P + \nabla\left((\mu + \mu_t) \cdot \left(\nabla V + (\nabla V)^{\tau}\right)\right) \tag{2}$$

These equations are supplemented by the corresponding equations of the turbulence model [12]. The calculations were carried out using the turbulence model (kinetic energy of turbulence k – ε, where ε is dissipation rate), in which the turbulent viscosity μ_t is determined by following expression:

$$\mu_t = C_\mu \cdot \rho \cdot \frac{k^2}{\varepsilon} \tag{3}$$

$$C_\mu = 0.09 \tag{4}$$

Standard wall functions are used on the wall.

The numerical method [13,14] is realized on a rectangular mesh with local adaptation and mesh resolution in areas with complex geometry of the mesh computational domain. In the radial clearance zone, the "gap cells" method is used to replace the Navier-Stokes equation with the Poiseuille equation.

To combine numerical solutions in the rotor and stator of the pump, the sliding mesh method is used. The transfer of flow parameters from the rotating to the stationary calculation area is carried out by a special interface "sliding surface", which provides interpolation of the flow parameters taking into account the "virtual" angular displacement of the meshes.

Fig. 3.shows the computational mesh of the second adaptation level for the AVS. The border of the sliding surface between the fixed mesh and the inducer is highlighted in blue color.

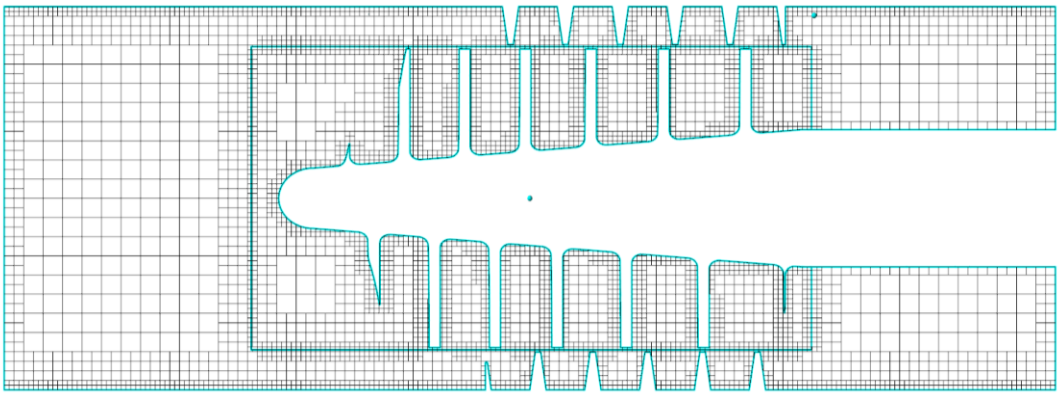

Fig.3. The computational mesh of the second adaptation level for the AVS

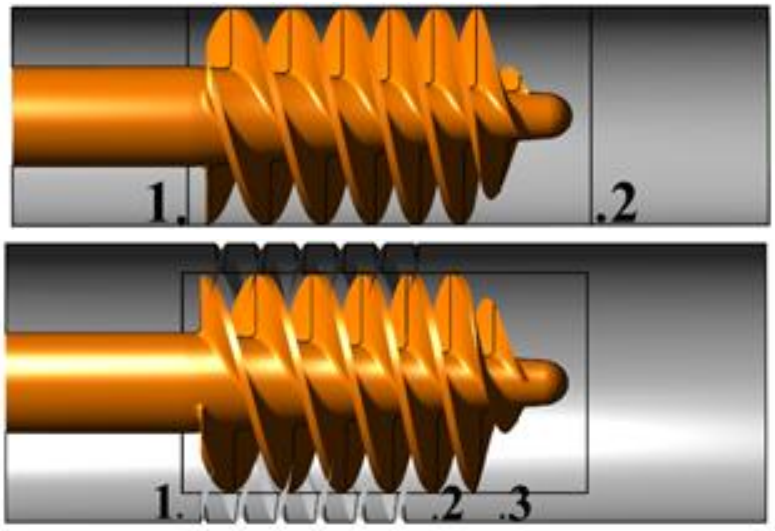

a) inducer

b) AVS

Fig.4. The selected points of pressure pulsations recording a) inducer b) AVS

Numerical modeling is carried out using the direct non-stationary method with the development of a solution from zero initial conditions to a quasi-stationary mode of operation, the output of which is controlled by the value of head. Typically, this mode is achieved within ten to fifteen full revolutions of the rotor. Data on pressure pulsations at selected points of the flow part are recorded after reaching the stationary mode.

The size of the computational mesh was around 500,000 cells, the time step of calculation was 4.4 e-5 s.

Results of numerical simulation of pressure pulsations in an inducer and AVS

The calculations were carried out at the optimum flow rate. For AVS, the results differ at different points. At the periphery, in the area of the fixed cascade of the AVS, there are zones of recirculation vortex flow.

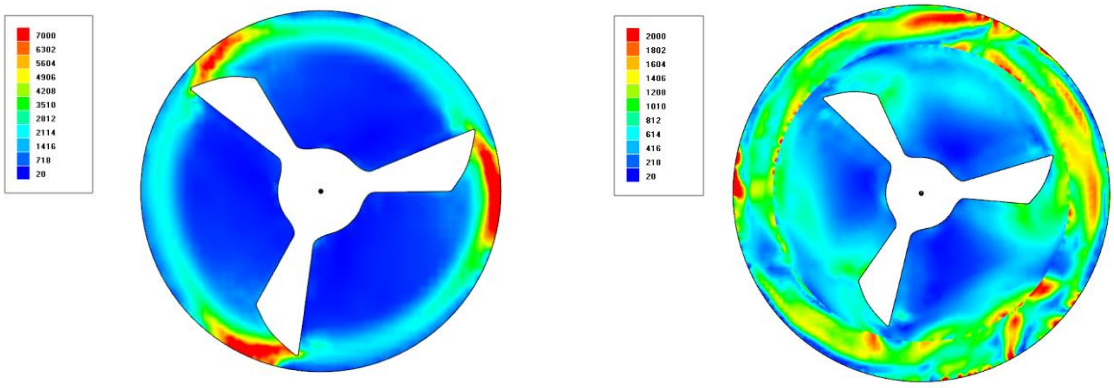

Fig. 5. Instant input vorticity field

Such velocity field inhomogeneity is also reflected in the inhomogeneity of the pressure field, especially at the periphery of the input part of the AVS. An inhomogeneous field of velocities and pressures generates random low-frequency pressure fluctuations at the input of the upstream AVS stage, which are well fixed at point 2 (Fig. 5). When moving away from the inlet of the stator channels, the low-frequency oscillations decrease, the discrete component of the blade passing frequency (BPF) of the inducer and its second harmonic prevail in the spectrum.

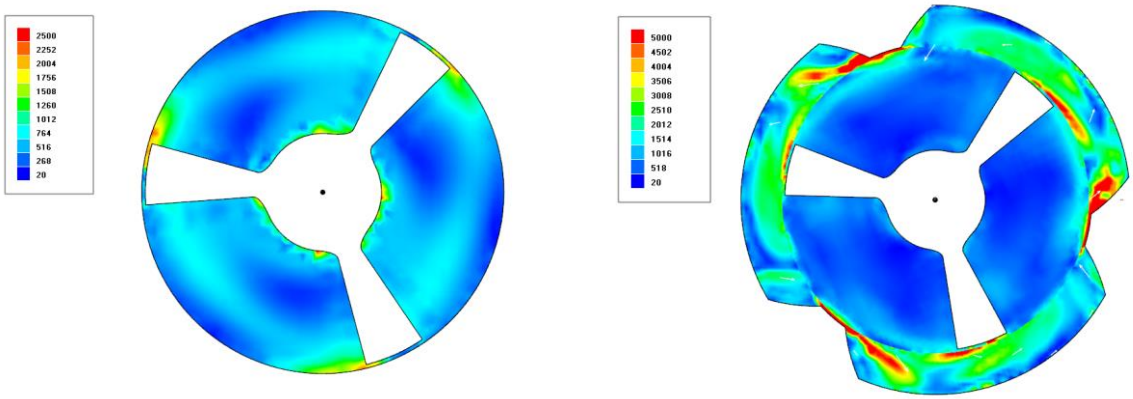

Fig. 6. Instant output vorticity field

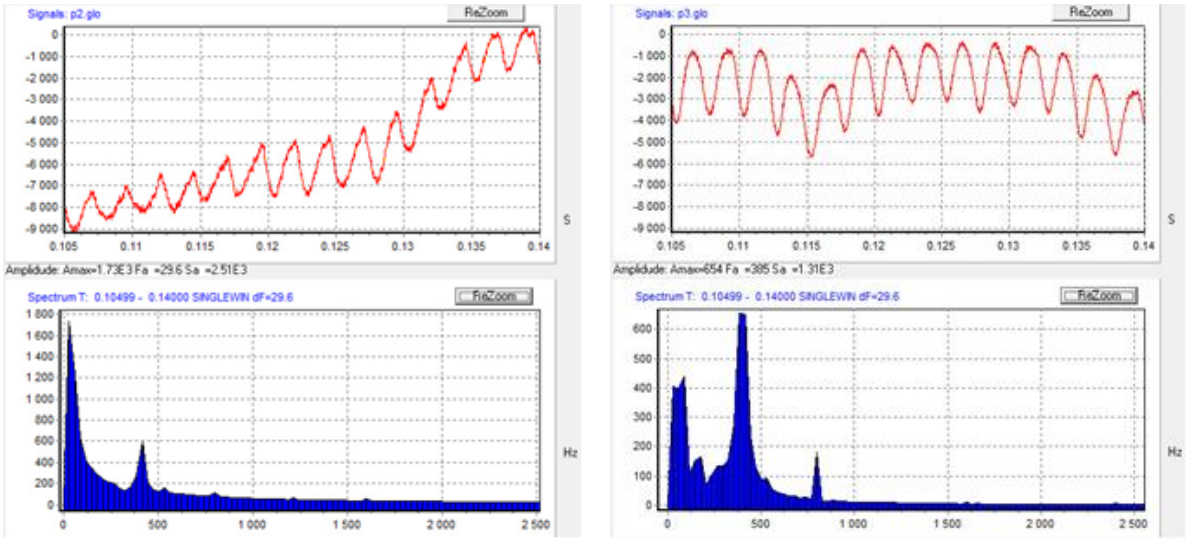

Fig. 7. Pressure pulsations at the inlet of the AVS at point 2 (on the left) and point 3

An analysis of the velocity and pressure fields in different sections of the flow part of the inducer and an AVS shows more equilibrium pressure distribution over the inducer blade grid in an AVS. This ensures a decrease in the BPF of the inducer at the outlet of the AVS compared with an single inducer almost in 2 times.

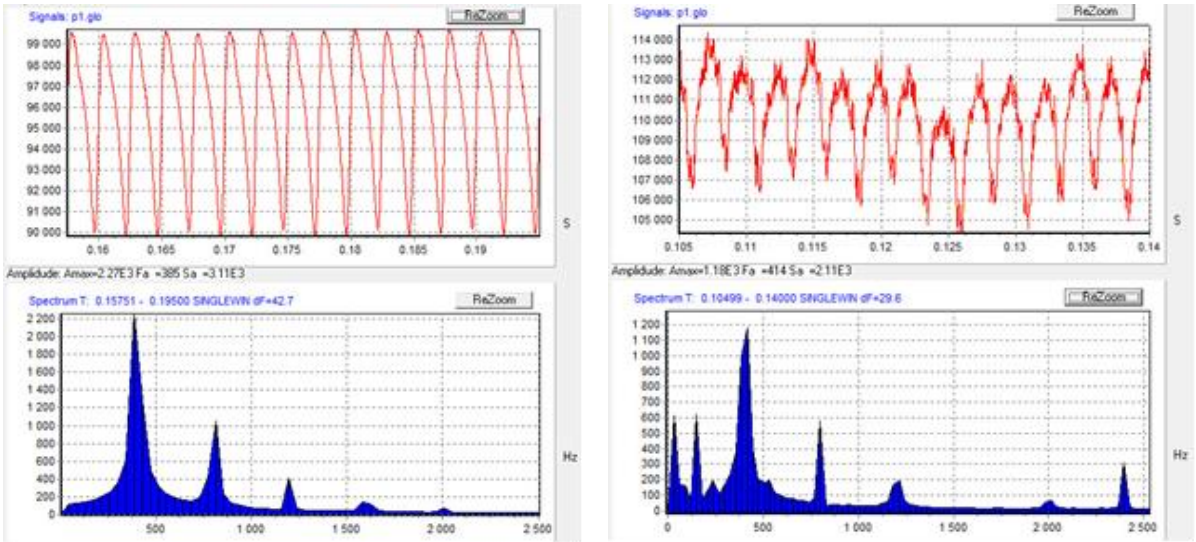

Fig.8. Pressure pulsations at the outlet of inducer (on the left) and AVS

Discussions

In the spectrum of pressure pulsations of the AVS at the inlet, low-frequency oscillations are recorded, which are provoked by vortex disturbances when the flow enters on the fixed cascade vanes. Oscillations at the shaft speed are also observed, which is explained by the circular asymmetry of the pressure field due to the interaction of the rotor with the fixed vane cascade of the AVS. Further studies of these phenomena are needed to optimize the position and number of vanes of the fixed cascade of the AVS.

List of reference

[1] Zotov B. N., Ankudinov A. A. Axial vortex pump. RF patent 2014509.
[2] Ankudinov A. A., Kirillov A. A. Improving the technical characteristics of the feed pump using an axial vortex stage. A look into the future — 2007. Materials NTK SPb: Publishing house of FSUE "Central Design Bureau MT" Rubin ", 2007.
[3] Ankudinov A. A., Zubov A. A., Misiagina IU. IU. Automated calculation and design of an axial vortex pump stage: a manual. — M.: Publishing house of BMSTU, 2017. — 44 p.
[4] Ankudinov A. A., Kuftov A. F. Energy characteristics of an axial vortex pump // News of Universities. — M.: Mechanical Engineering, No. 2, 1989.
[5] Ankudinov A. A. Calculation and design of the upstream axial vortex stage of a centrifugal pump: a Training manual. — M.: Publishing house of BMSTU, 2003. — 64 p.
[6] Ankudinov A. A., Turkova L.A. The use of the upstream axial vortex stage in the pumps of the Kaluga Turbine Plant. // Current status and development prospects of hydraulic engineering in the 21st century. // Proceedings of MNTK. —SPb: Publishing house of SPbSPU, 2003.
[7] Golubev A. I. Labyrinth screw pumps and seals for aggressive environments. — 2nd ed., Revised. and add. — M.: Mechanical Engineering, 1981. — 112 p.
[8] A Protopopov and V Vigovskij 2019 IOP Conf. Ser.: Mater. Sci. Eng. 492 012003
[9] N Egorkina and APetrov 2019 IOP Conf. Ser.: Mater. Sci. Eng. 492 012015
[10] V Lomakin and O Bibik 2019 IOP Conf. Ser.: Mater. Sci. Eng. 492 012037
[11] V Cheremushkin and V Lomakin 2019 IOP Conf. Ser.: Mater. Sci. Eng. 492 012039
[12] Wilcox, D. C., (1994) “Turbulence modeling for CFD” // DCW Industries, Inc. 460 p.
[13] Software package for gas and fluid flow simulation FlowVision. Version 2.5.0. Manual CAPVIDIA, 1999-2007 Leuven, Belgium
[14] FlowVision User's manual. TESIS LLC, 1999-2017, Moscow